

EMI Sensitivity Study and Mitigation Method of multi-GHz RF Cable and Connector

Abstract—A mobile system transmitting intermediate frequency/radio frequency (IF/RF) signals via a cable between Printed Circuit Boards (PCBs) can be vulnerable to electromagnetic interference (EMI), which may result from the connector itself as well as the interface between the connector and the cable. In this paper, the radiation physics of an RF cable and connector is comprehensively analyzed using a commercially available electromagnetic (EM) simulation tool. The sensitivity of EMI to a connector's physical dimension is studied. Based on the sensitivity study, a mitigation solution is proposed to reduce current leakage from the connector and cable interface by adopting the hot bar soldering technique.

Index Terms—Electromagnetic interference; RF connector; EMI mitigation methods, radiation physics, flex printed circuit, hot bar soldering.

I. INTRODUCTION

MOBILE system supporting multiple communication standards needs to contain antennas at multiple locations inside a mobile phone. A cable can be a good option for low loss signal transmission over long distances to connect antennas and mother PCB board together. However, an RF connector between a cable and a PCB can be a potential weak point from where current can leak out, spreading along the outer surface of the cable and resulting in electromagnetic radiation by the connector itself as well as the interface between the cable and motherboard. This EMI radiation may be problematic, particularly when the signal's spectrum contains high-frequency components. Governmental and standards bodies have promulgated limits on the EMI radiation from a system. For example, the Federal Communications Commission (FCC) has promulgated 47 C.F.R. 15.427, which includes a limit on emission from unintentional radiation of 500 $\mu\text{V}/\text{m}$ for unwanted emission at frequencies higher than 960 MHz. As the frequency of signals transmitted using RF connectors increases, the unintentional radiation emitted by such connectors generally increases. Accordingly, there is a need to reduce the unintentional radiation emitted by RF connectors, particularly for devices transmitting high-frequency signals.

Fig. 1 shows a general block diagram of a mobile system. This system includes a flexible printed cable (FPC) connected to the left and right-hand side PCBs with RF connectors. Communication chips are mounted on each PCB and connected through transmission lines to the connectors. Non-ideal transitions from/to the connectors can be potential EMI sources, for example, currents that get onto the FPC external surface be effectively radiated. This paper discusses such radiation physics and shows the EMI sensitivity to a connector's physical dimension. Finally, a mitigation solution is proposed and validated using EMI simulation.

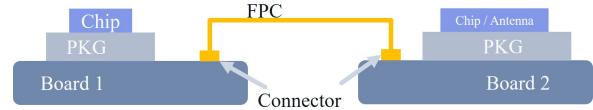


Fig. 1: Block diagram of RF interconnect.

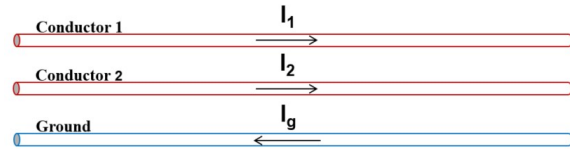


Fig. 2: Currents in multiconductor systems.

II. RADIATION PHYSICS

A. Common Mode Current

Fig. 2 shows a multiconductor system having two signal conductors and one ground conductor. Common-mode current or antenna-mode current is defined as shown in (1). This definition is used for measurement and EM modeling of the radiated emissions. Common-mode current, which is considerably lower in magnitude than differential-mode current, can produce a significant radiated electric field due to the fact that the emissions of the common-mode current are superimposed [1].

$$I_{cm} = I_1 + I_2 - I_g \quad (1)$$

High-speed digital serial interfaces employ differential signaling which can reduce the impact of return path discontinuities on EMI. Such interfaces use the transmission-line-mode (TL-mode) [1] as the primary mode of propagation. Under this TL-mode, the sum of the currents flow through signal and reference conductors is zero. If the time skew between the differential signaling conductors is significant, or the signal edges on the two conductors are significantly different, then common-mode current can be generated to such an extent as to create an EMI issue. Common-mode or antenna-mode currents of considerably less magnitude than differential-mode currents can produce the same level of radiated electric field.

Radiation of a single-ended RF signal can be explained by considering the antenna mode current. The antenna-mode signal is converted from TL-mode signal typically at the interface of two structures. It can be quantified by the difference of the imbalance factor and the TL-mode signals at the interface [2] - [5] as follows:

$$V_{AM} = \Delta h \times V_{TL-M} \quad (2)$$

Here V_{AM} is the antenna mode voltage and:

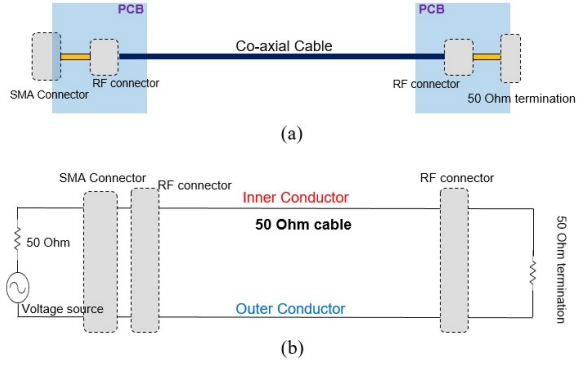


Fig. 3: Scheme of RF channel with RF connectors and coaxial cable.

$$\Delta h = h_2 - h_1 \quad (3)$$

Where h_1 and h_2 are the imbalance factor of two structures, respectively. Those two factors can be calculated from self-capacitance or inductance values [2]-[4].

Fig.3 (a) depicts a simple RF interconnect which is utilized as a test case in our study. It consists of two test boards, two RF connectors, two SMA connectors, and a 50Ω coaxial cable. In other scenarios, a coaxial cable may be replaced by FPC. The left-hand side SMA connector is connected to a signal source. The right-hand side SMA connector is terminated with 50Ω load. To eliminate SMA connectors' impact, it is assumed that there is no gap between the SMA connector and the PCB so no current will be leaked out. Fig. 3 (b) depicts a conceptual block diagram of the test case where the inner conductor and outer conductor of the coaxial cable are displayed separately.

Fig.4 is an equivalent circuit diagram of Fig. 3 (b) in which the connectors are replaced by impedance discontinuities caused by signal transition imperfections. (Time-domain reflectometer (TDR) results will illustrate this discontinuity in the next section.) I_{in} is the current flow through the inner conductor of the coaxial cable. $I_{return-cable}$ is the current flow along both the internal side and the external side of the outer conductor of the coaxial cable. Note that I_{in} is not necessarily equal to $I_{return-cable}$ due to $I_{return-displacement}$ which is the current through the impedance $Z_{radiation}$. The larger the impedance discontinuities are, the larger the value of $I_{return-displacement}$. The common-mode current in this equivalent circuit, I_{cm} , can be calculated by using:

$$I_{cm} = I_{in} - I_{return-cable} \quad (4)$$

Even a very small amount of antenna mode current following along the coaxial cable or FPC can cause significant radiation that will fail EMI specification. Fig. 5 shows a typical 3 meter EMI test setup in an anechoic chamber. An equivalent antenna mode current with several uA of the device under test (DUT) will generate large enough radiation to fail the EMI test.

A repeatedly-used model to predict or quickly calculate antenna-mode emissions is based on the fields of the simple Hertzian dipole or infinitesimal current element shown in Fig. 6

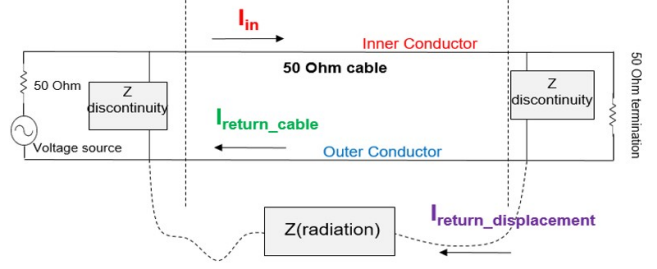


Fig. 4: Schematic of RF interconnect with impedance discontinuity.

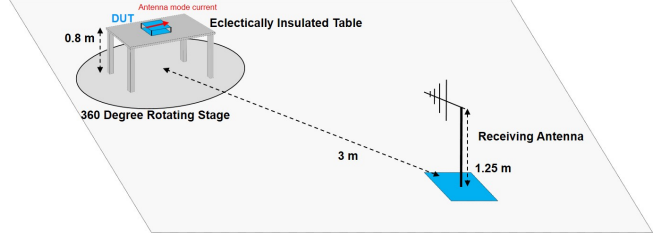


Fig. 5: Schematic of antenna model current caused radiation measurement.

The Hertzian dipole model is an extreme simplification and several dipole models need to be cascaded to form a more accurate model if other wire-type interconnects are multi-wavelength long and the wire-type interconnects have very thin cross-section [6]. Nevertheless, the Hertzian dipole model can be used to show how antenna-mode current generates radiations. The radiated electric field is given by:

$$E_r = 2 \frac{Il}{4\pi} \eta_0 \beta_0^2 \cos\theta \left(\frac{1}{\beta_0^2 r^2} - j \frac{1}{\beta_0^3 r^3} \right) e^{-j\beta_0 r} \quad (5)$$

$$E_\theta = \frac{Il}{4\pi} \eta_0 \beta_0^2 \sin\theta \left(j \frac{1}{\beta_0 r} + \frac{1}{\beta_0^2 r^2} - j \frac{1}{\beta_0^3 r^3} \right) e^{-j\beta_0 r} \quad (6)$$

$$E_\phi = 0 \quad (7)$$

where the intrinsic impedance of free space is given by $\eta_0 = \sqrt{\frac{\mu_0}{\epsilon_0}} = 120\pi$, and the phase constant β_0 is $\beta_0 = \omega \sqrt{\mu_0 \epsilon_0} = \frac{2\pi}{\lambda_0}$.

The maximum electric field strength can be written as:

$$E_{C_{max}} = j \frac{60Ilf}{\mu_0 r} e^{-j \frac{2\pi r}{\lambda_0}} \quad (8)$$

$$E_{C_{max}} = j 2\pi \times 10^{-7} \left(\frac{fIl}{r} \right) e^{-j\beta_0 r} \quad (9)$$

Then antenna mode current can be calculated by rearrange (9):

$$\left| \vec{I}_c \right|_{max} = \frac{\left| \vec{E}_{C,max} \right| \times r}{6.283 \times 10^{-7} \times f \times L} \quad (10)$$

Antenna mode current on cables can be a significant contributor to radiated emissions and these currents are not at all simple to predict. It is a simple matter to generate antenna-mode currents on cables, and those radiated emissions can easily exceed the EMC regulatory limits or intra-system EMI specifications.

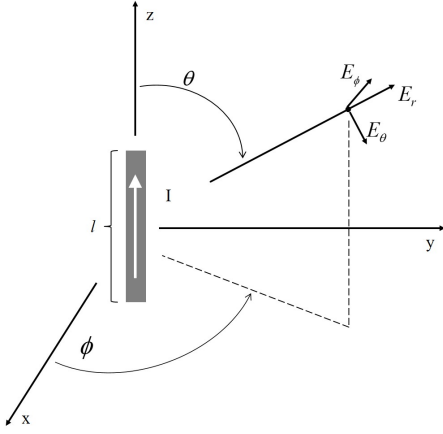


Fig. 6: The simple model of Hertzian dipole.

B. Antenna Realized Gain

To evaluate the EMI performance of IF/RF interconnects, those interconnects can be treated as an effective EMI antenna with sufficient electrical extent. Common mode or antenna mode current is the driven current flowing along the interconnects. To ensure at all directions those interconnects don't generate strong enough fields to desense other RF components or cause intra-system EMI failure, the realized gain of the formed antenna should be calculated and regulated. The realized gain of an antenna is calculated by considering the total efficiency of the antenna, along with its directivity. The total efficiency of the antenna considers the losses due to reflections at the input terminals as well as losses within the structure of the antenna.

Total efficiency e_0 may be written as:

$$e_0 = e_r \times e_c \times e_d \quad (11)$$

Where e_r is the reflection efficiency, e_d is the dielectric efficiency and e_c is the conduction efficiency. The dielectric and conduction efficiencies are usually grouped and known as e_{cd} . Total efficiency then becomes:

$$e_0 = e_r \times e_{cd} = e_{cd}(1 - |\Gamma|^2) \quad (12)$$

Where Γ is the reflection coefficient. The realized gain is calculated using the total efficiency and the directivity as follows:

$$G_0(dB) = 10 \log_{10}(e_0 D_0) \quad (13)$$

If the maximum realized gain of the IF/RF interconnect is smaller than a certain level, then intra-system EMI can be assured to be risk free.

III. SIMULATION AND MEASUREMENT RESULTS

This section discusses the correlation between the simulation and measurement results of the test case described in the previous section to build confidence in the analysis method. It also discusses the impedance imbalance contribution to common mode current along with the resulting radiation.

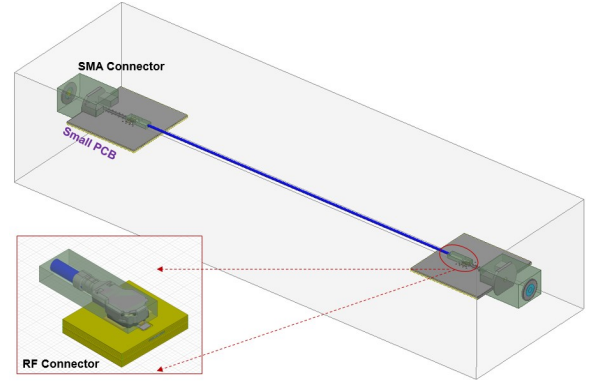


Fig. 7: RF channel with RF connectors and coaxial cable in HFSS.

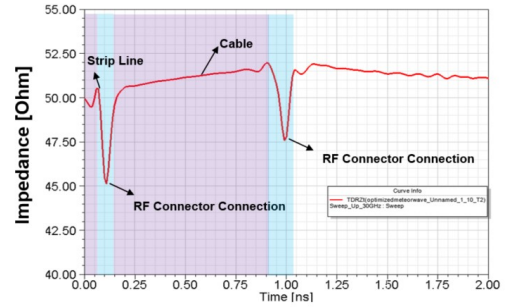


Fig. 8: TDR of RF channel with RF connectors and co-axial cable.

Far-field EMI simulation was done using a commercial EM analysis tool. Fig. 7 shows details of the modeled structure. Measurements were 3-m far-field emission measurements conducted in the anechoic chamber. RG58 cable was used to connect the left-hand side SMA connector to a signal generator. The right-hand side SMA connector was terminated using 50 Ohm termination. Besides the emission measurement, TDR measurement was also performed to quantify the impedance discontinuity of the DUT.

The transition between an RF connector and PCB is not electrically perfect, therefore there is parasitic capacitance or inductance. The TDR plot in Fig. 8 illustrates that the RF connector has a lower impedance of 45 Ohm relative to the coaxial cable's impedance of 50 Ohm. This impedance discontinuity leads to non-TEM mode electromagnetic fields and concomitant common-mode current. A portion of the current flows along the external surface of the connector to the outer conductor of the cable and the top layer of PCB. Even if the coaxial cable itself has good shielding effectiveness, this current can flow on the external surface of the outer conductor. If there is not a good return path for this current, then it will become displacement current and cause radiation.

The length of the coaxial cable is equivalent to several wavelengths at 10 GHz and the cable with RF connectors can be an effective radiator. Surface current density is plotted on top of the PCB and along the connector and coaxial cable's surface as shown in Fig. 9. Several valley points are labeled along the co-axial cable in Fig.9.

The correlation of simulated and measured radiation results

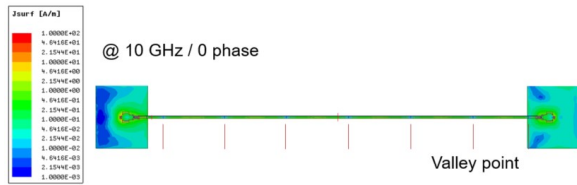


Fig. 9: Current distribution of RF channel with RF connectors and co-axial cable.

TABLE I: RETOTAL CORRELATION

Frequency [GHz]	rETotal [dBuV/m]			
	Simulation	Measurement	Delta	Spec
7.5	76	72	4.4	54
10	77	77	0	54

is shown in Table I; good correlation is observed at the frequencies of interest. The data show that both simulated and measured results do not pass the specification of 54 dBuV/m at 3 m [7]. Thus, an effective solution is needed to suppress radiation from the connector and cable, as will be addressed in the next section.

IV. EMI SENSITIVITY STUDY AND RADIATION MITIGATION TECHNIQUES

As stated in section III, if there is an impedance discontinuity between portions of an RF channel and there are gaps of the connector's ground shield, the common mode current will be generated and leaks out to the outer surface of the co-axial cable or FPC. Now, the question is, "How can radiation caused by common mode current be mitigated in a channel having RF connectors and cable?" This paper analyzes the sensitivity of EMI to the RF connector's physical dimension and proposes an EMI mitigation method by using the hot bar soldering technique. The key concept is to reduce the current that leaks through to the external surface of the outer conductor of the coaxial cable or FPC. If the coaxial cable or FPC is long enough, the leaked current can result in a considerable amount of radiation.

A. Sensitivity of EMI to Connector's Ground Gaps

Fig. 10 shows the side view of an IF/RF interconnect including PCB, FPC and the board to board connector (B2B connector). When signal is transmitting through this interconnect, three types of current flowing along the interconnect namely functional current, return current, and the common-mode current. The sidewall of the connector's ground shield should have a good connection between the PCB ground plane and the FPC's outer conductor. Why does such a shield work? It works because it provides a path for the return current to flow on the inside of the shield rather than leaking out onto the PCB. Even with a considerable impedance discontinuity, the common-mode current along the cable becomes very small because the return current is confined inside the shield and on the inside of the FPC outer conductor. Nevertheless, with mechanical constraints, ground gaps along the shield are unavoidable thus it's necessary to conduct a study of the

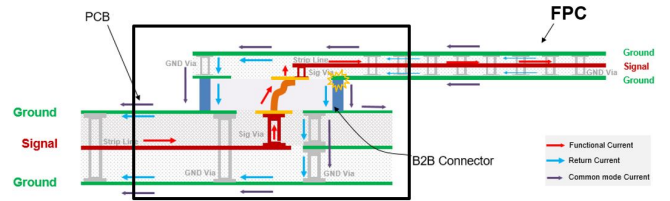


Fig. 10: Scheme of current flowing and leakage

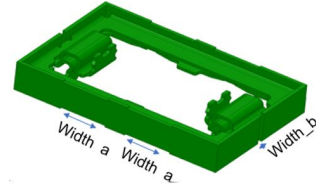


Fig. 11: Ground shield of B2B connector

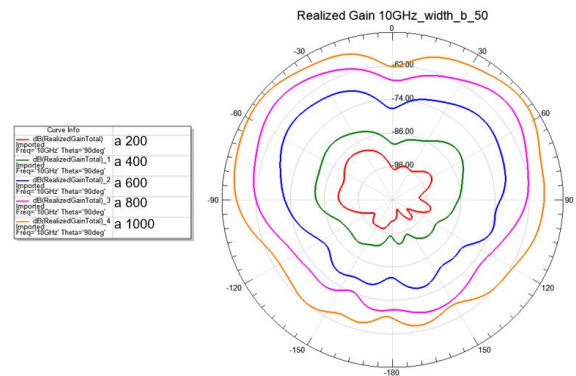


Fig. 12: EMI sensitivity to width a

EMI sensitivity to the connector's physical dimension of those ground gaps. As shown in Fig. 11, there are two holes with width a on the front and back side of the connector's ground shield and there is one ground hole with width b on both left and right side of the ground shield of the connector. In this study, the width a varies from 200 um to 1000 um with step 200 um. Width b sweeps from 50 um to 200 um with step 50 um.

Fig. 12 shows the 2D plot of realized gain at 10 GHz with width b fixed at 50 um while varying width a from 200 um to 1000 um. Table.II lists the realized gain results at different frequency points comparing scenarios varying width a while keep width b fixed at 50 um. It clearly shows that realized gain is sensitive to variable width a . The maximum realized gain increases as width a get larger.

TABLE II: EMI SENSITIVITY TO WIDTH A

Width a [um]	Maximum Realized Gain [dB]			
	1 GHz	2 GHz	3 GHz	4 GHz
200	-147	-132	-108	-87
400	-134	-115	-94	-79
600	-119	-99	-80	-65
800	-110	-90	-70	-55
1000	-103	-83	-62	-50

Fig. 13 shows the surface current density at 5 GHz on the top surface of ground plane with different width a and width b . Yellow trace shown in the picture is the IF signal trace. Comparing Fig. 13 (a) and Fig. 13 (b), width a is fixed and width b varies from 50 μm to 100 μm , current leakage from the left and right ground gap is very small. Fig. 13 (c) and Fig. 13 (d) show the same trend. Fig. 13 (a)(b)(c)(d) illustrate current get leaked out most along the bottom edge of the ground shield which is at the same side of the IF signal net. This means EMI is most sensitive to the bottom edge of the ground shield from where the functional current is flowing in and out.

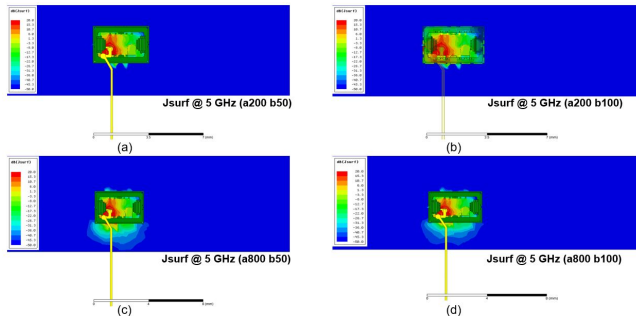


Fig. 13: Current distribution with different width a and width b

B. EMI Mitigation By Using Hot Bar Technique

Pulsed heat thermode (Hot Bar) soldering is a joining technology where two pre-tinned parts are heated to the melting point of the tin. The joining technology results in a permanent electro-mechanical joint. The hot bar technique can be used to make a good connection between the FPC and the PCB and eliminate the usage of a board-to-board (B2B) connector. As shown in Fig. 14, FPC and PCB are directly soldered together. IF/RF trace is routed on the inner layer of the PCB and onto the FPC through a short via. Without the B2B connector used, this configuration can provide a smooth signal transition along with better EMI performance. Fig. 15 shows insertion loss and return loss of the FPC-via-PCB interconnect. After optimization, return loss of this interconnect is less than -25 dB up to 10 GHz which means the signal transition is smooth. Realized gain results depicted in Fig. 16 proves that interconnect constructed by hot bar soldering has small radiation.

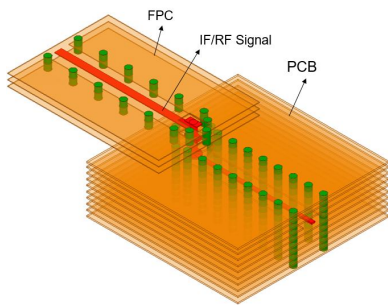


Fig. 14: 3D view of a stack-card PCB configuration

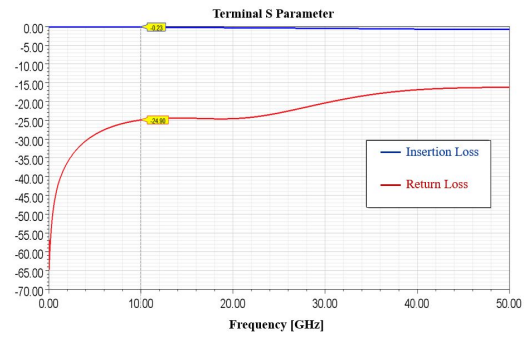


Fig. 15: Insertion loss and return loss of IF/RF interconnect

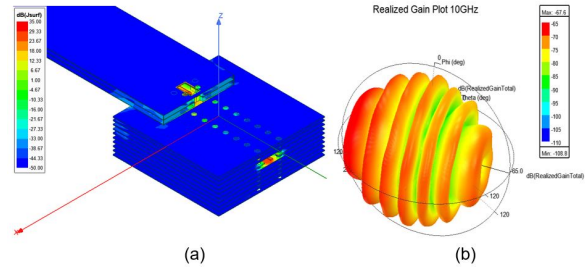


Fig. 16: (a) Surface current density of ground plane of FPC and PCB; (b) Realized gain plot at 10 GHz

V. CONCLUSION

This paper has presented results showing a good correlation of far-field radiation between simulations and measurements of a mobile system having RF connectors and a coax cable. Both measurement and simulation results demonstrated that a sufficiently long RF coax cable with connectors can be a potential EMI antenna. It can be concluded that a realistic impedance imbalance can produce common-mode current and these current flows along the external surface of the coaxial cable's outer conductor. Radiation caused by this common-mode current can violate the far-field specification and an effective mitigation solution is necessary. One mitigation solution using the hot bar technique has been proposed and demonstrated.

ACKNOWLEDGMENT

The author would like to thank Gerardo R. Luevano, Sang-June Park and Tim Michalka for their invaluable contributions in this work.

REFERENCES

- [1] A. Vukicevic, F. Rachidi, M. Rubinstein and S.V. Tkachenko, "On the evaluation of antenna-mode currents along transmission lines", *IEEE Trans. Electromagn., Compat.*, vol. 48, no. 4, pp. 693-700, August 2017.
- [2] T. Watanabe, O. Wada, T. Miyashita, and R. Koga, "Common-mode current generation caused by difference of unbalance of transmission lines on a printed circuit board with narrowground pattern". *IEICE Trans. Commun.*, vol. E83-B, no. 3, pp. 593-599, Mar. 2017.
- [3] C. Su and T.H. Hubing, "Imbalance difference model for common-mode radiation from printed circuit boards". *IEEE Trans. Electromagn. Compat.*, vol. 53, no. 1, pp. 150-156, Feb. 2011.
- [4] Y. Toyota, K. Iokibe, R. Koga, and T. Watanabe, "Mode-equivalent modelling of system consisting of transmission lines with different imbalance factors.", *Proc. Asia-Pacific Int. Symp. Electromagn. Compat.*, pp. 676-679, May. 2011.

- [5] H. Kwak and T. H. Hubing, "Investigation of the imbalance difference model and its application to various circuit board and cable geometries," *Proc. IEEE Int. Symp. Electromagn. Compat.*, pp. 273-278, Pittsburgh, Aug. 2012.
- [6] C. R. Paul and S. A. Nasar, "Introduction to Electromagnetic Fields", 2nd ed., McGraw Hill, 1987, pp.502-508.
- [7] T. Wang, S. Park, G. R. Romo and T. Michalka, "radiation mechanisms and mitigation methods in multi-GHz RF cable and connector for next generation mobile applications", *2018 IEEE Symp. Electromagn. Compat. SIPI* pp. 245-249, Oct. 2018.